Six-degree-of-freedom Plate Paper

Thomas H. Vose Paul Umbanhowar Kevin M. Lynch

***Abstract*— We show that arbitrary small amplitude periodic motion of a rigid plate causes isolated point parts on the plate to move as if they are in a position-dependent velocity field. By allowing the plate to vibrate with six-degrees-of-freedom, we can create a large family of programmable velocity fields. Several fields in this family exhibit sink and source behavior, opening up the possibility of using a single rigid plate for sensorless part orientation, uncertainty-reducing transport, and simultaneous manipulation of multiple parts. The fields are verified experimentally with a device that can generate user-defined plate motions with up to six-degrees-of-freedom.**

I. Introduction

In this paper we show that the motion of an isolated point part sliding on an oscillating rigid plate is well approximated by a position-dependent velocity field.

II. Related Work

III. Kinematics

A. Plate Kinematics

Consider a rigid plate undergoing small amplitude vibration. We define three coordinate systems: a fixed inertial frame $\mathcal{W}$, a local frame $\mathcal{S}$ attached to the origin of the plate, and an inertial frame $\mathcal{S}'$ instantaneously aligned with $\mathcal{S}$ (Figure 1). The z-axis of $\mathcal{W}$ is in the direction opposite the gravity vector, which is represented as $\mathbf{g} = [0, 0, -g]^T$ in the $\mathcal{W}$ frame. The z-axis of $\mathcal{S}$ is always perpendicular to the plate surface.

We choose to specify plate motions in the $\mathcal{W}$ frame in terms of the linear acceleration of the origin of the plate $\ddot{\mathbf{p}} = [\ddot{p}_x, \ddot{p}_y, \ddot{p}_z]$ and the angular acceleration of the plate $\boldsymbol{\alpha} = [\alpha_x, \alpha_y, \alpha_z]$. All six acceleration components must be periodic with period T. When the linear and angular accelerations are integrated, the plate's linear velocity $\dot{\mathbf{p}}$, angular velocity $\boldsymbol{\omega}$, and configuration must be continuous and periodic with period T. The configuration of the plate in $\mathcal{W}$ is given by

$$\begin{bmatrix} \mathbf{R} & \mathbf{p} \\ 0 & 1 \end{bmatrix} \in SE(3),$$

where $\mathbf{R} \in SO(3)$.

B. Part Kinematics

Let P be a point part with mass m in contact with the plate. As illustrated in Figure 1, we let $\mathbf{q} = [x_{\mathcal{S}}, y_{\mathcal{S}}, 0]^T$ be a vector in $\mathcal{S}$ to P, and $\mathbf{r} = [x, y, z]^T$ be a vector in $\mathcal{W}$ to P such that

$$\mathbf{r} = \mathbf{p} + \mathbf{R}\mathbf{q}. \tag{1}$$

Let P^* be the point on the plate directly underneath P. The position of P^* is given by the vector $\mathbf{r}^* = \mathbf{r}$ in the $\mathcal{W}$ frame.

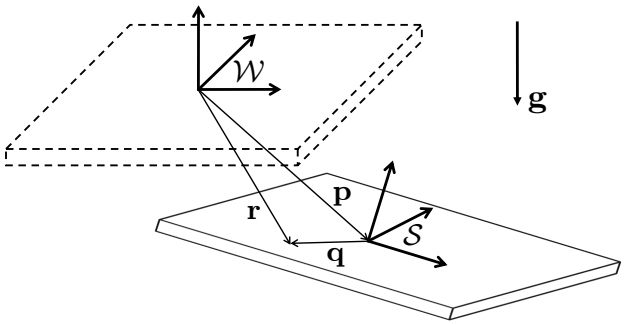

Fig. 1. An extremely exaggerated picture of the plate displaced from the fixed $\mathcal{W}$ frame by the vector $\mathbf{p}$. The $\mathcal{S}$ frame is always attached to the origin of the plate. The position of the part is given by $\mathbf{r}$ in the $\mathcal{W}$ frame and by $\mathbf{q}$ in $\mathcal{S}$ frame.

The velocity and acceleration of P^* in the $\mathcal{W}$ frame are given by

$$\dot{\mathbf{r}}^* = \dot{\mathbf{p}} + \boldsymbol{\omega} \times \mathbf{R}\mathbf{q} \tag{2}$$

$$\ddot{\mathbf{r}}^* = \ddot{\mathbf{p}} + \boldsymbol{\omega} \times \boldsymbol{\omega} \times \mathbf{R}\mathbf{q} + \boldsymbol{\alpha} \times \mathbf{R}\mathbf{q}. \tag{3}$$

The velocity and acceleration of P in the $\mathcal{W}$ frame are given by

$$\dot{\mathbf{r}} = \dot{\mathbf{r}}^* + \mathbf{R}\dot{\mathbf{q}} \tag{4}$$

$$\ddot{\mathbf{r}} = \ddot{\mathbf{r}}^* + 2\boldsymbol{\omega} \times \mathbf{R}\dot{\mathbf{q}} + \mathbf{R}\ddot{\mathbf{q}}. \tag{5}$$

IV. Part Dynamics

A. System Model

Up to three forces may act on the part: gravity, friction, and the normal force from the plate (Figure 2). Applying Newton's second law in the $\mathcal{S}'$ frame gives

$$\mathbf{f}_{\mathrm{N}_{\mathcal{S}'}} + \mathbf{f}_{\mathrm{F}_{\mathcal{S}'}} + \mathbf{f}_{\mathrm{G}_{\mathcal{S}'}} = m\mathbf{R}^T\ddot{\mathbf{r}} \tag{6}$$

$$= m\mathbf{R}^T\left(\ddot{\mathbf{r}}^* + 2\boldsymbol{\omega} \times \mathbf{R}\dot{\mathbf{q}}\right) + m\ddot{\mathbf{q}}, \tag{7}$$

where $\mathbf{f}_{\mathrm{N}_{\mathcal{S}'}} = [0, 0, N]^T$, $\mathbf{f}_{\mathrm{F}_{\mathcal{S}'}} = [F_{x_{\mathcal{S}}}, F_{y_{\mathcal{S}}}, 0]^T$, and $\mathbf{f}_{\mathrm{G}_{\mathcal{S}'}} = m\mathbf{R}^T\mathbf{g}$ are the normal, frictional, and gravitational forces on the part in the $\mathcal{S}'$ frame. Solving (6) for $\ddot{\mathbf{r}}$ yields an expression for the part's acceleration in the $\mathcal{W}$ frame:

$$\ddot{\mathbf{r}} = \frac{1}{m}\mathbf{R}\left(\mathbf{f}_{\mathrm{N}_{\mathcal{S}'}} + \mathbf{f}_{\mathrm{F}_{\mathcal{S}'}}\right) + \mathbf{g}. \tag{8}$$

Explicit expressions for $\mathbf{f}_{\mathrm{N}_{\mathcal{S}'}}$ and $\mathbf{f}_{\mathrm{F}_{\mathcal{S}'}}$ are derived in the following two sections.

The state vector $\mathbf{x}_{\mathcal{W}} = [\mathbf{r}, \dot{\mathbf{r}}]^T$ can be computed by integrating (8). Alternatively, the state vector $\mathbf{x}_{\mathcal{S}} = [\mathbf{q}, \dot{\mathbf{q}}]^T$ can be computed from $\mathbf{x}_{\mathcal{W}}$ noting that (1) and (4) imply

$$\mathbf{q} = \mathbf{R}^T\left(\mathbf{r} - \mathbf{p}\right) \tag{9}$$

$$\dot{\mathbf{q}} = \mathbf{R}^T\left(\dot{\mathbf{r}} - \dot{\mathbf{r}}^*\right). \tag{10}$$

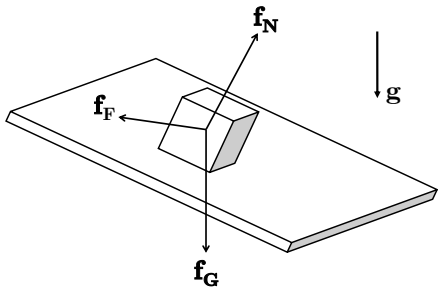

Fig. 2. The three forces that may act on the part are due to gravity, friction, and the the contact with the plate. The gravitational force $\mathbf{f}_G$ always acts in the negative z-direction of the $\mathcal{W}$ frame, the frictional force $\mathbf{f}_F$ always acts tangent to the plate surface, and the normal force $\mathbf{f}_N$ always acts perpendicular to the plate surface.

Our analysis is restricted to situations where the part always remains in contact with the plate. Contact is maintained as long as the magnitude of the normal force is positive. Additionally, contact implies the acceleration of the part perpendicular to the plate surface is zero at all times in the $\mathcal{S}$ frame. Mathematically, we express this as

$$\mathbf{z}^\circ \ddot{\mathbf{q}} = 0, \tag{11}$$

where $\mathbf{z}^\circ \triangleq [0, 0, 1]$.

B. Normal Force

Pre-multiplying (7) by $\mathbf{z}^\circ$ and noting (11) yields the following expression for the magnitude of the normal force, N:

$$N = m\mathbf{z}^\circ \mathbf{R}^T \left(\ddot{\mathbf{r}}^* + 2\boldsymbol{\omega} \times \mathbf{R}\dot{\mathbf{q}} - \mathbf{g}\right). \tag{12}$$

We define the *effective gravity* as

$$g_{\text{eff}} = \mathbf{z}^\circ \mathbf{R}^T \left(\ddot{\mathbf{r}}^* + 2\boldsymbol{\omega} \times \mathbf{R}\dot{\mathbf{q}} - \mathbf{g}\right), \tag{13}$$

so that

$$N = m g_{\text{eff}}. \tag{14}$$

C. Friction Force

We assume Coulomb friction in our model. Since frictional forces can only act in the x-y plane of the $\mathcal{S}'$ frame we define the matrix

$$\mathbf{S}_{XY} \triangleq \begin{bmatrix} 1 & 0 & 0 \\ 0 & 1 & 0 \\ 0 & 0 & 0 \end{bmatrix},$$

that projects vectors onto the x-y plane.

The frictional force acting on a part located at $\mathbf{r}$ depends on the state of the system:

- If the part is moving relative to the plate, the frictional force is directed opposite the relative velocity vector $\dot{\mathbf{q}}$. The magnitude of the force is the product of the coefficient of kinetic friction and the magnitude of the normal force acting on the part.
- If the part is at rest with respect to the plate, the frictional force acts in the same direction as the acceleration of P^* projected onto the plane of the plate surface. There are two possibilities for the magnitude of the frictional force. If the magnitude of the acceleration of P^* projected onto the plane of the plate surface is greater than the product of the coefficient of static friction and the effective gravity at $\mathbf{r}$, the magnitude of the frictional force is equal to the product of the coefficient of static friction and the normal force acting on the part. If the magnitude of the acceleration of P^* projected onto the plate of the plate surface is less than or equal to the product of the coefficient of static friction and the effective gravity at $\mathbf{r}$, the magnitude of the frictional force is equal to the product of the part's mass and the magnitude of the acceleration of P^* projected onto the plane of the plate surface.

Mathematically, we summarize these cases as

$$\mathbf{f}_{\mathrm{F}_{\mathcal{S}'}} = \begin{cases} -\mu_k N \dfrac{\dot{\mathbf{q}}}{\|\dot{\mathbf{q}}\|}, & \|\dot{\mathbf{q}}\| > 0; \\ \mu_s N \dfrac{\mathbf{S}_{XY}\mathbf{R}^T\ddot{\mathbf{r}}^*}{\|\mathbf{S}_{XY}\mathbf{R}^T\ddot{\mathbf{r}}^*\|}, & \|\dot{\mathbf{q}}\| = 0 \\ & \|\mathbf{S}_{XY}\mathbf{R}^T\ddot{\mathbf{r}}^*\| > \mu_s g_{\text{eff}}; \\ m\mathbf{S}_{XY}\mathbf{R}^T\ddot{\mathbf{r}}^*, & \|\dot{\mathbf{q}}\| = 0 \\ & \|\mathbf{S}_{XY}\mathbf{R}^T\ddot{\mathbf{r}}^*\| \le \mu_s g_{\text{eff}}; \end{cases} \tag{15}$$

where μ_k and μ_s are the respective kinetic and static coefficients of friction between the part and the plate.

D. Simplified System Model

For the type of plate motions we wish to implement, we assume that the part is sliding at all times. We also assume that the linear and angular displacements of the plate during each cycle are insignificant, implying that the $\mathcal{W}$ and $\mathcal{S}'$ frames are indistinguishable. Mathematically, we express this as

$$\mathbf{p} \approx \mathbf{0} \qquad \mathbf{R} \approx \mathbf{I},$$

where $\mathbf{I}$ is the identity matrix. It follows that the part's position vector in the $\mathcal{W}$ frame can be approximated as $\mathbf{r} \approx \mathbf{q} = [x, y, 0]^T$, and that the gravitational, frictional, and normal forces on the part can be considered aligned with the $\mathcal{W}$ axes.

Let the plane of x and y velocities in the $\mathcal{W}$ frame be called $\mathcal{V}_{xy}$ and the plane of x and y accelerations in the $\mathcal{W}$ frame be called $\mathcal{A}_{xy}$. With the assumptions above, the approximate acceleration of the part in $\mathcal{A}_{xy}$ is obtained by simplifying the x and y components of (8):

$$\begin{bmatrix} \ddot{x} \\ \ddot{y} \\ 0 \end{bmatrix} = S_{XY}\ddot{\mathbf{r}} \approx -\mu_k g_{\text{eff}} \frac{\dot{\mathbf{q}}}{\|\dot{\mathbf{q}}\|}. \tag{16}$$

The effective gravity g_{eff} and the relative velocity vector $\dot{\mathbf{q}}$ that respectively dictate the magnitude and direction of the part's acceleration in $\mathcal{A}_{xy}$ can be approximated by simplifying (13) and (10):

$$g_{\text{eff}} \approx \mathbf{z}^\circ \left(\ddot{\mathbf{r}}^* + 2\boldsymbol{\omega} \times \dot{\mathbf{q}} - \mathbf{g}\right) \tag{17}$$

$$\approx \mathbf{z}^\circ \left(\ddot{\mathbf{p}} + \boldsymbol{\omega} \times \boldsymbol{\omega} \times \mathbf{r} + \boldsymbol{\alpha} \times \mathbf{r} + 2\boldsymbol{\omega} \times \dot{\mathbf{q}} - \mathbf{g}\right) \tag{18}$$

$$\dot{\mathbf{q}} \approx \mathbf{S}_{XY}\left(\dot{\mathbf{r}} - \dot{\mathbf{r}}^*\right) \tag{19}$$

$$\approx \mathbf{S}_{XY}\left(\dot{\mathbf{r}} - \dot{\mathbf{p}} - \boldsymbol{\omega} \times \mathbf{r}\right). \tag{20}$$

V. Asymptotic Velocity

Simulations show that for a given periodic plate motion and position $\mathbf{r}$ on the plate, there is a unique average velocity $\mathbf{v}_{\mathrm{a}}(\mathbf{r})$ such that a point part at $\mathbf{r}$, moving with any other average velocity, tends toward $\mathbf{v}_{\mathrm{a}}(\mathbf{r})$. We call $\mathbf{v}_{\mathrm{a}}(\mathbf{r})$ the *asymptotic velocity at* $\mathbf{r}$. Thus a part's motion on the plate is given approximately by the position-dependent *asymptotic velocity field*, where the quality of the approximation depends on the rate of convergence to the asymptotic velocity at each location. For plate motions that adhere to the assumptions of the simplified system model given in the previous section, simulations show there is a rapid convergence to the asymptotic velocity during which time the displacement is negligible.

Theorem1: For an arbitrary periodic plate motion there is a unique asymptotic velocity for an isolated point part located at $\mathbf{r}$ assuming that the part does not displace from $\mathbf{r}$, the part is always slipping, and friction is the only force acting on the part in the plane of the plate surface.

Proof: In the $\mathcal{V}_{xy}$ plane let the velocity of the plate at $\mathbf{r}$ be given by $\mathbf{v}^* = S_{XY}\dot{\mathbf{r}}^*$. For periodic plate motions, $\mathbf{v}^*$ sweeps out a closed loop over the course of a cycle. Let P_1 and P_2 be two point parts located at $\mathbf{r}$ with identical coefficients of kinetic friction, μ_k. Let the velocities of P_1 and P_2 in $\mathcal{V}_{xy}$ be $\mathbf{v}_1 = S_{XY}\dot{\mathbf{r}}_1$ and $\mathbf{v}_2 = S_{XY}\dot{\mathbf{r}}_2$. Let $\Delta v = \|\mathbf{v}_1 - \mathbf{v}_2\|$ be the distance between $\mathbf{v}_1$ and $\mathbf{v}_2$ in $\mathcal{V}_{xy}$.

From (16), P_1 and P_2 always accelerate with equal magnitude in the direction of $\mathbf{v}^*$ (Figure 3). It follows that $\frac{d}{dt}(\Delta v) \leq 0$. The nondecreasing case where $\frac{d}{dt}(\Delta v) = 0$ corresponds to $\mathbf{v}_1$, $\mathbf{v}_2$, and $\mathbf{v}^*$ being collinear such that $\mathbf{v}^*$ is not between $\mathbf{v}_1$ and $\mathbf{v}_2$. However, the periodic motion of the plate ensures that there will always be at least one instant of time during the cycle when $\mathbf{v}_1$, $\mathbf{v}_2$, and $\mathbf{v}^*$ are not collinear, or $\mathbf{v}_1$, $\mathbf{v}_2$, and $\mathbf{v}^*$ are collinear such that $\mathbf{v}^*$ is between $\mathbf{v}_1$ and $\mathbf{v}_2$. In either case, $\frac{d}{dt}(\Delta v) < 0$ during this instant.

Since the initial velocities of P_1 and P_2 are arbitrary, all parts located at $\mathbf{r}$ must converge to a unique closed trajectory in $\mathcal{V}_{xy}$ that we call the *asymptotic trajectory at* $\mathbf{r}$. The average velocity of the points on the asymptotic trajectory at $\mathbf{r}$ is the unique asymptotic velocity at $\mathbf{r}$. QED.

Corollary: In the $\mathcal{V}_{xy}$ plane the asymptotic trajectory at $\mathbf{r}$ lies within the convex hull of the plate's trajectory at $\mathbf{r}$.

Proof: HOW TO PROPERLY WRITE PROOF??????????

Theorem2: The asymptotic trajectory is periodic with a period equal to the period of the plate.

Proof: HOW TO PROVE?????????

Since the asymptotic trajectory has a period of T in $\mathcal{V}_{xy}$, we formally define the asymptotic velocity as

$$\mathbf{v}_{\mathrm{a}}(\mathbf{r}) = \frac{1}{T}\int_{t}^{t+T} \dot{\mathbf{r}}dt \quad \text{such that} \quad \dot{\mathbf{r}}(t) = \dot{\mathbf{r}}(t+T),$$

where $\mathbf{r}$ is kept fixed.

For simple plate motions, assumptions can sometimes be made that allow the asymptotic velocity field to be approximated analytically [**?**], [**?**]. Otherwise, it can be determined numerically by computing the asymptotic velocity at a discrete set of points on the plate as follows:

- Set the part's initial velocity to zero.
- Use (16) to simulate the part dynamics (without updating the position) for one cycle of plate motion.
- If the velocity at the end of the cycle is greater than a very small predefined tolerance ϵ of the initial velocity (i.e., if $\dot{\mathbf{r}}(t+T) - \dot{\mathbf{r}}(t) > \epsilon$), simulate another cycle in which the part's initial velocity is equal to its final velocity from the previous cycle.
- Repeat the previous two steps M times until the velocity difference between the beginning and end of the cycle is less than ϵ.

The value of MT is a measure of the rate of convergence to the asymptotic state. As long as $MT \ll 1$ s, the asymptotic velocity provides a good model of part motion. As a point of reference, the twelve asymptotic velocity fields in Figure 5 correspond to plates that oscillate with a period of $T = 0.03$ s; every point in all twelve fields satisfies $MT \leq 0.12$ s for $\epsilon = 0.001$ m/s. Figure 4 shows in detail how two parts at one particular location converge to an asymptotic trajectory on a plate undergoing the motion generating the `Whirlpool` field in Figure 5(h).

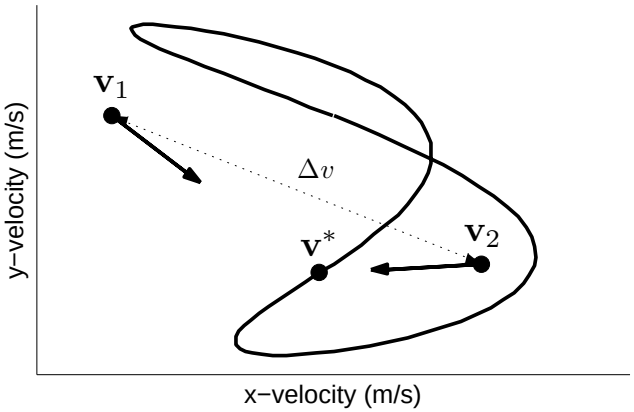

Fig. 3. The $\mathcal{V}_{xy}$ plane at an arbitrary location $\mathbf{r}$ in which the velocity of the plate $\mathbf{v}^*$ sweeps out a closed trajectory. At any given instant, the velocity of a part (e.g., $\mathbf{v}_1$) is changing in the direction of $\mathbf{v}^*$. AHHH–HOW TO DESCRIBE??? GET RID OF (M/S) LABELS

VI. Estimating Asymptotic Velocity Fields for Sinusoidal Plate Motions

A. Sinusoidal Motion Primitives

In this paper we confine ourselves to linear and angular accelerations with sinusoidal components that all have the same frequency, f:

$$\begin{aligned} \ddot{p}_x &= A_x \sin(2\pi f t + \phi_x) & \alpha_x &= A_\theta \sin(2\pi f t + \phi_\theta) \\ \ddot{p}_z &= A_z \sin(2\pi f t + \phi_z) & \alpha_y &= A_\varphi \sin(2\pi f t + \phi_\varphi) \\ \ddot{p}_y &= A_y \sin(2\pi f t + \phi_y) & \alpha_z &= A_\psi \sin(2\pi f t + \phi_\psi). \end{aligned}$$

We refer to plate accelerations of this form as *sinusoidal motion primitives*.

B. Simplified Transient Acceleration Model

Let a point part located at $\mathbf{r}$ be initially at rest in the $\mathcal{W}$ frame. Barring the exceptional case (***should trajectory be

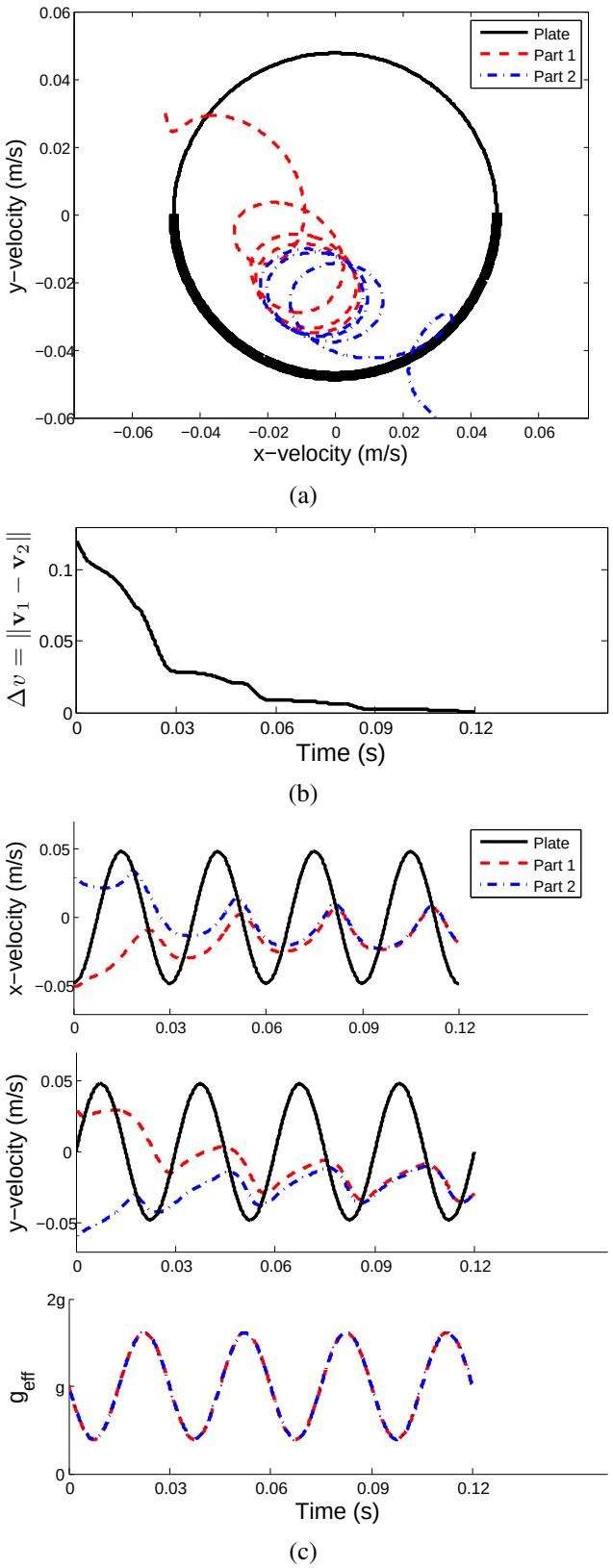

Fig. 4. The trajectories in $\mathcal{V}_{xy}$ of a plate undergoing the motion specified in Figure 5(h) and two parts with initial velocities of $(-0.05, 0.03)$ m/s and $(0.03, 0)$ m/s. All trajectories correspond to four cycles of plate motion with period $T = 0.03$ s at the location $(0.06, 0)$ m are shown in (a). Both parts rapidly approach a nearly circular asymptotic trajectory centered around $(-0.01, -0.025)$ m/s that is fully contained within the plate's trajectory. The distance between the parts' velocities in $\mathcal{V}_{xy}$ never increases and rapidly approaches zero as shown in (b). In the top two graphs of (c) the x and y-components of the velocity are plotted individually; in the bottom graph of (c) the effective gravity is plotted. ADD (M/S) LABEL TO B.

defined in x-y-t space to clarify that staring on trajectory in $\mathcal{V}_{xy}$ does not necessarily mean you on the trajectory?****), there is a transient period during the first few cycles of plate motion in which the part converges to the asymptotic trajectory at $\mathbf{r}$. During the transient period the average acceleration of the part is nonzero in order to bring the average cycle velocity closer to the asymptotic velocity. Thus, to a good approximation, the asymptotic velocity at $\mathbf{r}$ is proportional to the average transient acceleration at $\mathbf{r}$. To estimate the part's average transient acceleration we use the acceleration model given by (16), but further simplify the expressions for g_{eff} and $\dot{\mathbf{q}}$ given by (18) and (20).

Let $\|\ddot{\mathbf{p}}\|_\infty = \ddot{p}_{\max}$ and $\|\boldsymbol{\alpha}\|_\infty = \alpha_{\max}$. Assuming the part's initial speed is less than the maximum speed of the plate, a sinusoidal motion primitive imposes the following tight bounds: $\|\dot{\mathbf{q}}\|_\infty \leq \frac{\ddot{p}_{\max} T}{\pi}$ and $\|\boldsymbol{\omega}\|_\infty \leq \frac{\alpha_{\max} T}{2\pi}$. We choose to bound the part's position in our transient acceleration model such that $\|\mathbf{r}\|_\infty \leq \frac{g}{\alpha_{\max}}$. Thus, we can bound (18) as follows:

$$g_{\text{eff}} \leq g\left(\frac{\ddot{p}_{\max}}{g} + \frac{\alpha_{\max} T^2}{4\pi^2} + 1 + \frac{\alpha_{\max}\ddot{p}_{\max} T^2}{\pi^2} + 1\right) \quad (21)$$

If we choose to operate our system such that $\ddot{p}_{\max} \leq 10$ m/s^2, $\alpha_{\max} \leq 100$ rad/s^2, and $T \leq 0.05$ s, the second and fourth terms of (21), corresponding to the centripetal and Coriolis accelerations, are the least significant. Ignoring these terms reduces (18) to

$$g_{\text{eff}} \approx \mathbf{z}^\circ\left(\ddot{\mathbf{p}} + \boldsymbol{\alpha} \times \mathbf{r} - \mathbf{g}\right) = \ddot{p}_z + \alpha_x y - \alpha_y x + g \quad (22)$$

To simplify $\dot{\mathbf{q}}$, we make the highly exaggerated assumption that during the transient period the plate's velocity in the plane of the plate is much greater than the part's velocity in the plane of the plate (i.e., $\mathbf{S}_{XY}\dot{\mathbf{r}} \ll \mathbf{S}_{XY}\dot{\mathbf{r}}^*$). Thus, (20) reduces to

$$\dot{\mathbf{q}} \approx \mathbf{S}_{XY}\left(-\dot{\mathbf{r}}^*\right) = \mathbf{S}_{XY}\left(-\dot{\mathbf{p}} - \boldsymbol{\omega} \times \mathbf{r}\right) = \begin{bmatrix} -\dot{p}_x - \omega_z y \\ -\dot{p}_y + \omega_z x \\ 0 \end{bmatrix}. \quad (23)$$

We make the important observation that in this grossly simplified transient acceleration model, $g_{\text{eff}} = g_{\text{eff}}(\ddot{p}_z, \alpha_x, \alpha_y)$ and $\dot{\mathbf{q}} = \dot{\mathbf{q}}(\dot{p}_x, \dot{p}_y, \omega_z)$. Thus, the *magnitude* of the part's acceleration in the plane of the plate is a function of $\ddot{p}_z$, α_x, and α_y, and the *direction* of the part's acceleration in the plane of the plate is a function of $\dot{p}_x$, $\dot{p}_y$, and ω_z. We refer to $\ddot{p}_z$, α_x, and α_y as the *out-of-plane acceleration components*. Out-of-plane acceleration components come directly from the sinusoidal motion primitive. We refer to $\dot{p}_x$, $\dot{p}_y$, and ω_z as the *in-plane velocity components*. In-plane velocity components can be obtained by integrating the *in-plane acceleration components* $\ddot{p}_x$, $\ddot{p}_y$, and α_z of the sinusoidal motion primitive.

C. Estimating Asymptotic Velocity

We now make a final exaggerated assumption that the acceleration of the part in $\mathcal{A}_{xy}$ is negligible when $g_{\text{eff}} < g$. This means that we assume the frictional force is too weak to accelerate the part when the plate is accelerating downwards (i.e., in the negative z-direction). Thus, the average magnitude

of the part's acceleration in $\mathcal{A}_{xy}$ during the transient period is roughly proportional to the average value of g_{eff} during the half of the cycle when $g_{\text{eff}} > g$. Because g_{eff} is a sinusoid shifted by g, this average is roughly proportional to the amplitude of g_{eff}. Similarly, the average direction of the part's acceleration $\mathcal{A}_{xy}$ during the transient period roughly corresponds to the average direction of $\dot{\mathbf{q}}$ during the half of the cycle when $g_{\text{eff}} > g$.

For example, consider the scenario in Figure 3. In (a), we see that the plate sweeps out a circular trajectory in $\mathcal{V}_{xy}$. In (c), we see that the amplitude of g_{eff} is roughly $0.5g$, and that $g_{\text{eff}} > g$ only when the plate's y-velocity is negative (we also show this in (a) using a thicker line to denote the portion of the plate's trajectory when $g_{\text{eff}} > g$). Based on the simplified transient acceleration model, the direction of the asymptotic velocity should correspond to the average direction of the plate's velocity in $\mathcal{V}_{xy}$ when $g_{\text{eff}} > g$. Thus, the asymptotic velocity should have a negative y-component and no x-component. This is very nearly true—the asymptotic trajectory to which the parts are converging in (a) has an average y-velocity that is negative and an average x-velocity that is very close to zero, although slightly negative.

If the amplitude of g_{eff} were to decrease, we would expect the magnitude of the asymptotic velocity to decrease. In $\mathcal{V}_{xy}$ this corresponds to a translation of the asymptotic trajectory in the positive y-direction. In the extreme case when the amplitude of g_{eff} is zero, we would expect the asymptotic trajectory to be centered on the origin and the asymptotic velocity to be zero.

If the amplitude of g_{eff} were to increase, we would expect the magnitude of the asymptotic velocity to increase. In $\mathcal{V}_{xy}$ this corresponds to a translation of the asymptotic trajectory in the negative y-direction. In the extreme case when the amplitude of g_{eff} is g (if the amplitude of g_{eff} becomes greater than g the part loses contact with the plate and the model is no longer valid), the asymptotic trajectory may become tangent to the plate's trajectory, but it must remain within the convex hull of plate's trajectory.

VII. Asymptotic Velocity Fields Arising from Sinusoidal Motion Primitives

Though simple, sinusoidal motion primitives generate a variety of asymptotic velocity fields. Throughout this section we look at several classes of sinusoidal motion primitives and explain how to estimate the corresponding asymptotic velocity field from the simplified transient acceleration model. The exact fields, calculated numerically, are shown in Figure 5. Approximate equations governing each field are given in Table I.

A. Combining In-Plane Translation with Out-of-Plane Translation: Translational Fields

The class of *translational* sinusoidal motion primitives combine the in-plane acceleration components $\ddot{p}_x$ and $\ddot{p}_y$ with out-of-plane acceleration component $\ddot{p}_z$:

$$\begin{aligned}\ddot{p}_x &= A_x \sin(2\pi f t)\\ \ddot{p}_y &= A_y \sin(2\pi f t)\\ \ddot{p}_z &= A_z \sin(2\pi f t + \phi).\end{aligned}$$

From (22) and (23), the effective gravity and relative velocity vector can be written as

$$\begin{aligned} g_{\text{eff}} &\approx \ddot{p}_z + g = A_z \sin(2\pi f t + \phi) + g\\ \dot{\mathbf{q}} &\approx \begin{bmatrix} -\dot{p}_x \\ -\dot{p}_y \\ 0 \end{bmatrix} = \begin{bmatrix} \frac{A_x}{2\pi f}\cos(2\pi f t) \\ \frac{A_y}{2\pi f}\cos(2\pi f t) \\ 0 \end{bmatrix}. \end{aligned}$$

We note that neither g_{eff} nor $\dot{\mathbf{q}}$ is position-dependent, from which it follows that the transient acceleration will be identical at all locations, with a direction corresponding to $\pm(A_x, A_y)$ and a magnitude that scales with A_z.

Without loss of generality, let us consider the special case where $A_y = 0$ implying that $\dot{\mathbf{q}}$ is always aligned with the x-axis. If $\phi = \frac{3}{2}\pi$, g_{eff} and $\dot{\mathbf{q}}$ are out of phase with each other—i.e., the plate moves in the positive x-direction during the half of the cycle when $g_{\text{eff}} > g$. As illustrated in Figure 5(a), the asymptotic velocity field for this case corresponds to uniform motion in the positive x-direction. This is an example of a `Trans` field. In general, A_x, A_y, A_z, and ϕ can be controlled to set the desired magnitude and direction of the `Trans` field.

B. Combining In-Plane Rotation with Out-of-Plane Translation: Circular Fields

EXPAND??? —add pddx and pddy. then show how one can reduce motion to rotation about the point (-ay/alphaz, ax/aphaz).

The class of *circular* sinusoidal motion primitives combine the in-plane acceleration component α_z with the out-of-plane acceleration component $\ddot{p}_z$:

$$\begin{aligned}\alpha_z &= A_\psi \sin(2\pi f t)\\ \ddot{p}_z &= A_z \sin(2\pi f t + \phi)\end{aligned}$$

From (22) and (23), the effective gravity and relative velocity vector can be written as

$$\begin{aligned} g_{\text{eff}} &\approx \ddot{p}_z + g = A_z \sin(2\pi f t + \phi) + g\\ \dot{\mathbf{q}} &\approx \begin{bmatrix} -\omega_z y \\ \omega_z x \\ 0 \end{bmatrix} = \begin{bmatrix} \frac{A_\psi}{2\pi f}\cos(2\pi f t) y \\ -\frac{A_\psi}{2\pi f}\cos(2\pi f t) x \\ 0 \end{bmatrix}. \end{aligned}$$

We note that g_{eff} is position-independent, and that in a polar coordinate system $\dot{\mathbf{q}}$ points in the positive or negative angular direction at all locations. It follows that during the transient period parts will accelerate in a clockwise or counterclockwise direction with a magnitude that scales with A_z.

The orientation of the field depends on the phase ϕ. For example, if $\phi = \frac{3}{2}\pi$, g_{eff} and $\dot{\mathbf{q}}$ are out of phase with each other—i.e., the plate moves in the counterclockwise direction during the half of the cycle when $g_{\text{eff}} > g$. As illustrated in Figure 5(b), the asymptotic velocity field for this case corresponds to counterclockwise circular motion around the origin. We refer to this as a `Circle` field. In general, A_ψ, A_z, and ϕ can be controlled to set the desired magnitude and direction of the `Circle` field.

C. Combining In-Plane Translation with Out-of-Plane Rotation: Nodal Line Fields

The class of *nodal line* sinusoidal motion primitives combine the in-plane acceleration components $\ddot{p}_x$ and $\ddot{p}_y$ with the out-of-plane acceleration components α_x and α_y:

$$\begin{aligned}\ddot{p}_x &= A_x \sin(2\pi f t)\\ \ddot{p}_y &= A_y \sin(2\pi f t)\\ \alpha_x &= A_\theta \sin(2\pi f t + \phi)\\ \alpha_y &= A_\varphi \sin(2\pi f t + \phi).\end{aligned}$$

From (22) and (23), the effective gravity and relative velocity vector can be written as

$$\begin{aligned} g_{\text{eff}} &\approx \alpha_x y - \alpha_y x + g\\ &= A_\theta \sin(2\pi f t + \phi) y - A_\varphi \sin(2\pi f t + \phi) x + g\\ \dot{\mathbf{q}} &\approx \begin{bmatrix} -\dot{p}_x \\ -\dot{p}_y \\ 0 \end{bmatrix} = \begin{bmatrix} \dfrac{A_x}{2\pi f}\cos(2\pi f t) \\ \dfrac{A_y}{2\pi f}\cos(2\pi f t) \\ 0 \end{bmatrix}. \end{aligned}$$

We note that g_{eff} is position-dependent. Its amplitude increases with distance from the line through the origin in the direction of (A_θ, A_φ). We refer to this line as a nodal line. We also note that $\dot{\mathbf{q}}$ is position-independent and points in the direction of the vector (A_x, A_y). It follows that during the transient period parts will accelerate in a direction corresponding to $\pm(A_x, A_y)$ with a magnitude that scales with their distance from the nodal line.

Let us examine the special case where $A_y = A_\theta = 0$, implying that $\dot{\mathbf{q}}$ is always aligned with the x-axis and that the amplitude of g_{eff} increases with distance from the y-axis. Thus, we expect the magnitude of the transient acceleration to increase with distance from the y-axis. Further, when g_{eff} is greater than g on one side of the y-axis it is less than g on the other side. This introduces an asymmetry that causes the direction of the part's transient acceleration to differ on opposite sides of the y-axis. Depending on on the phase ϕ, a part will accelerate towards or away from the nodal line.

For example, if $\phi = \frac{3}{2}\pi$, g_{eff} and $\dot{\mathbf{q}}$ are out of phase with each other for positions satisfying $x < 0$—i.e., for parts with positive x-positions, the plate moves in the positive x-direction during the half of the cycle when $g_{\text{eff}} > g$. On the other hand, the plate moves in the negative x-direction during the half of the cycle when $g_{\text{eff}} > g$ for parts with positions satisfying $x > 0$. It follows that during the transient period parts with negative positions tend to get accelerated in the positive x-direction whereas parts with positive positions tend to get accelerated in the negative x-direction. As illustrated in Figure 5(c), the asymptotic velocity field for this case corresponds to a squeeze field converging on the y-axis. We refer to this as a `LineSink` field.

If $\phi = \frac{1}{2}\pi$, the asymptotic velocity field diverges from the y-axis as shown in Figure 5(d). We refer to this as a `LineSource` field. The full dynamics of `LineSink` and `LineSource` fields generated by "bang-bang" motion primitives are analyzed in [**?**].

In general, the class of nodal line sinusoidal motion primitives create a nodal line of zero velocity in the direction of the rotation axis (i.e., the direction of the vector (A_θ, A_φ)). The value of ϕ determines whether the nodal line is attractive or repulsive. As illustrated in Figure 5(d–f), A_x, A_y, A_θ, A_φ, and ϕ can be chosen to create fields such as `SkewSink`, `SkewSource`, and `ShearFlow`.

Closely related to all of these fields is the `DivCircle` field shown in Figure 5(g). This field has a nodal line that is both attractive and repulsive. It arises from the class of sinusoidal motion primitives that combine the in-plane acceleration component α_z with the out-of-plane acceleration components α_x and α_y:

$$\begin{aligned}\alpha_z &= A_\psi \sin(2\pi f t)\\ \alpha_x &= A_\theta \sin(2\pi f t + \phi)\\ \alpha_y &= A_\varphi \sin(2\pi f t + \phi).\end{aligned}$$

As with the other nodal line fields, the amplitude of g_{eff} increases with distance from the nodal line, and, g_{eff} is always larger than g on one side of the nodal line and smaller than g on the other side. What differentiates this field from the others is that $\dot{\mathbf{q}}$ always points in the positive or negative *angular* direction. Thus, parts on one side of the nodal line move clockwise whereas parts on the other side move counterclockwise.

D. Combining In-Plane Translation with Out-of-Plane Rotation: Nodal Fields

The class of *nodal* sinusoidal motion primitives combine the in-plane acceleration components $\ddot{p}_x$ and $\ddot{p}_y$ with the out-of-plane acceleration components α_x and α_y:

$$\begin{aligned}\ddot{p}_x &= A_x \sin(2\pi f t)\\ \ddot{p}_y &= A_y \cos(2\pi f t)\\ \alpha_x &= A_\theta \sin(2\pi f t + \phi)\\ \alpha_y &= A_\varphi \cos(2\pi f t + \phi),\end{aligned}$$

From (22) and (23), the effective gravity and relative velocity vector can be written as

$$\begin{aligned} g_{\text{eff}} &\approx \alpha_x y - \alpha_y x + g\\ &= A_\theta \sin(2\pi f t + \phi) y - A_\varphi \cos(2\pi f t + \phi) x + g\\ \dot{\mathbf{q}} &\approx \begin{bmatrix} -\dot{p}_x \\ -\dot{p}_y \\ 0 \end{bmatrix} = \begin{bmatrix} \dfrac{A_x}{2\pi f}\cos(2\pi f t) \\ -\dfrac{A_y}{2\pi f}\sin(2\pi f t) \\ 0 \end{bmatrix}. \end{aligned}$$

The relative velocity $\dot{\mathbf{q}}$ is position-independent with a constant magnitude and a direction that rotates at a constant rate. This implies that the part can potentially accelerate in any direction at any location. However, we can rule out many possibilities by examining g_{eff}. In particular, we expect the transient acceleration to be an odd function of position because $g_{\text{eff}}(x, y, t) = -g_{\text{eff}}(-x, -y, t)$. Further, the magnitude of the transient acceleration should increase with distance from the origin because the amplitude of g_{eff} increases in this manner.

TABLE I

APPROXIMATE FORM OF THE ASYMPTOTIC VELOCITY FOR THE FIELDS SHOWN IN FIGURE 5. CHECK EQUATIONS FOR MISMATCHES!!!!

Field Name	Asymptotic Velocity
`Trans`	$\mathbf{v}(x,y) \approx a(1,0)$
`Circle`	$\mathbf{v}(x,y) \approx a(-y,x)$
`LineSink`	$\mathbf{v}(x,y) \approx a(-x,0)$
`LineSource`	$\mathbf{v}(x,y) \approx a(x,0)$
`SkewSink`	$\mathbf{v}(x,y) \approx (-ax,-bx)$
`SkewSource`	$\mathbf{v}(x,y) \approx (ax,bx)$
`ShearFlow`	$\mathbf{v}(x,y) \approx a(0,x)$
`DivCircle`	$\mathbf{v}(x,y) \approx (axy,bx^2)$
`Sink`	$\mathbf{v}(x,y) \approx a(-x,-y)$
`Source`	$\mathbf{v}(x,y) \approx a(x,y)$
`Whirlpool`	$\mathbf{v}(x,y) \approx (-ax,-by)$
`Centrifuge`	$\mathbf{v}(x,y) \approx (ax,by)$

In general, nodal sinusoidal motion primitives create fields with a node of zero velocity at the origin of the plate. The value of ϕ determines whether the node is attractive or repulsive as well as whether the field is oriented clockwise or counterclockwise. The values of A_x, A_y, A_θ, and A_φ determine the strength and eccentricity of the field. As illustrated in Figure 5(h)–(k), nodal fields include `Sink`, `Source`, `Whirlpool`, and `Centrifuge` (and a second version of `Circle` which is not illustrated).

VIII. DESIGNING ASYMPTOTIC VELOCITY FIELDS

The primitive fields shown in Figure 5 represent a small subset of the class of asymptotic velocity fields obtainable with a six-DOF oscillating plate. In this section we look at two methods of generating more fields: concatenation and parameter optimization.

A. Concatenating Primitives

In theory, by rapidly sequencing primitive asymptotic velocity fields, the set of all convex combinations of primitive fields are obtainable. This can be done in practice by temporally concatenating the acceleration components of motion primitives. The resulting asymptotic velocity field loosely resembles a time-averaged superposition of the concatenated primitive fields. Two concatenated fields are shown in Figure 6. The `SqueezeTrans` field, which transports parts while simultaneously reducing their configuration uncertainty, results from concatenating the motion primitive for a `LineSink` field with the motion primitive for a `Trans` field. The `Saddle` field results from concatenating the motion primitive for a `LineSink` field with the motion primitive for a `LineSource` field.

********The `Jet` field results from concatenating two circular motion primitives whose centers of rotation are on opposite sides of the y-axis. TECHNICALLY WE CANNOT DO A JET SINCE CIRCLES SCALE WITH DISTANCE FROM ORIGIN*****

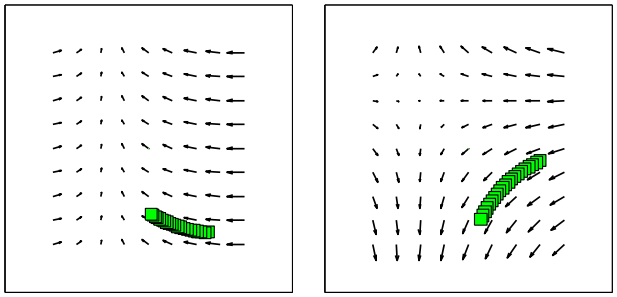

(a) `SqueezeTrans` (b) `Saddle`

Fig. 6. Asymptotic velocity fields from concatenated sinusoidal motion primitives.

Time-averaging the component fields only approximates the actual concatenated field because there is an interaction between the motion primitives depending on the order in which they are executed; the sliding motion at the end of one motion primitive influences the part's behavior during the next motion primitive. For example, the squeeze line of the `SqueezeTrans` field in Figure 6 is not centered on the y-axis as we would expect from time-averaging a `LineSink` field and a `Trans` field. This illustrates that there is some nonlinear interaction between the concatenated primitives. To lessen this effect, the motion primitives may be joined by a period during which the plate is at rest; however, this reduces the strength of the field.

B. Parameter Optimization

If a particular asymptotic velocity field is desired, a numerical routine can be used to find a plate motion that generates an approximation to the desired field (if one exists). This can be achieved by calculating the asymptotic velocity field for a particular plate motion at a discrete set of points and comparing it to the desired field. The plate motion is then altered in an effort to minimize the norm of the error.

A practical implementation might include parameterizing a simple class of plate motion. For example, the twelve free parameters (six amplitudes and six phases) of a sinusoidal motion primitives could be used. The algorithm would find the optimum values of the parameters within specified limits to best match the desired field. If these twelve parameters do not yield a sufficiently rich set of fields, more free parameters can be added to the acceleration components of the motion primitive. Ideally, a fairly small number of free parameters will be able to generate the vast majority of the set of all fields obtainable with a six-DOF plate.

IX. EXPERIMENTAL WORK

Our six-DOF vibratory device is shown in Figure **??**. The plate has a diameter of 10.5 inches and is made of $\frac{1}{2}$????? inch thick aluminum honeycomb. The plate is actuated from below by six speakers (****) evenly spaced along the perimeter of a circle. The speakers are driven by a stereo amplifier. Each

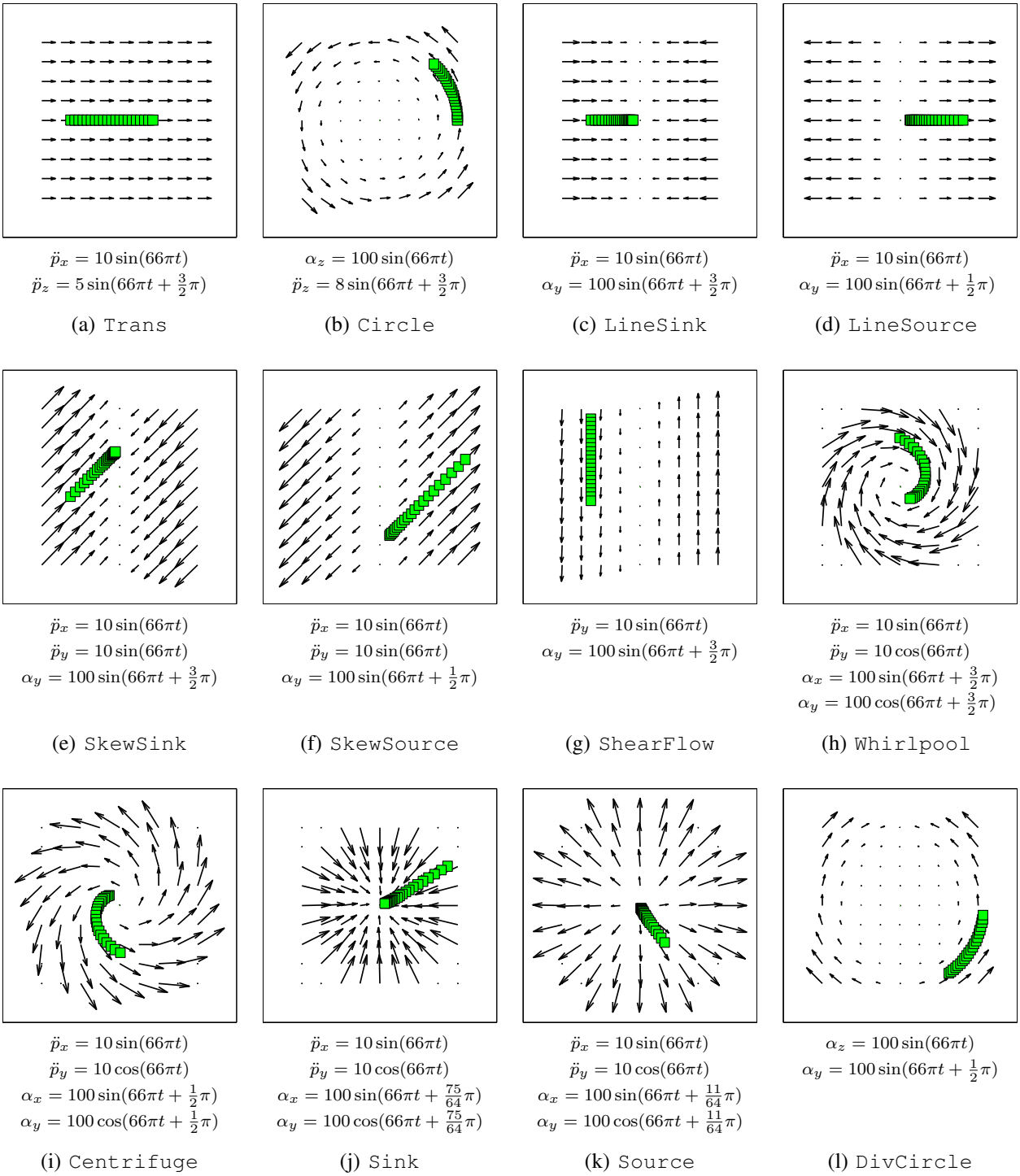

$\ddot{p}_x = 10\sin(66\pi t)$
$\ddot{p}_z = 5\sin(66\pi t + \frac{3}{2}\pi)$

(a) `Trans`

$\alpha_z = 100\sin(66\pi t)$
$\ddot{p}_z = 8\sin(66\pi t + \frac{3}{2}\pi)$

(b) `Circle`

$\ddot{p}_x = 10\sin(66\pi t)$
$\alpha_y = 100\sin(66\pi t + \frac{3}{2}\pi)$

(c) `LineSink`

$\ddot{p}_x = 10\sin(66\pi t)$
$\alpha_y = 100\sin(66\pi t + \frac{1}{2}\pi)$

(d) `LineSource`

$\ddot{p}_x = 10\sin(66\pi t)$
$\ddot{p}_y = 10\sin(66\pi t)$
$\alpha_y = 100\sin(66\pi t + \frac{3}{2}\pi)$

(e) `SkewSink`

$\ddot{p}_x = 10\sin(66\pi t)$
$\ddot{p}_y = 10\sin(66\pi t)$
$\alpha_y = 100\sin(66\pi t + \frac{1}{2}\pi)$

(f) `SkewSource`

$\ddot{p}_y = 10\sin(66\pi t)$
$\alpha_y = 100\sin(66\pi t + \frac{3}{2}\pi)$

(g) `ShearFlow`

$\ddot{p}_x = 10\sin(66\pi t)$
$\ddot{p}_y = 10\cos(66\pi t)$
$\alpha_x = 100\sin(66\pi t + \frac{3}{2}\pi)$
$\alpha_y = 100\cos(66\pi t + \frac{3}{2}\pi)$

(h) `Whirlpool`

$\ddot{p}_x = 10\sin(66\pi t)$
$\ddot{p}_y = 10\cos(66\pi t)$
$\alpha_x = 100\sin(66\pi t + \frac{1}{2}\pi)$
$\alpha_y = 100\cos(66\pi t + \frac{1}{2}\pi)$

(i) `Centrifuge`

$\ddot{p}_x = 10\sin(66\pi t)$
$\ddot{p}_y = 10\cos(66\pi t)$
$\alpha_x = 100\sin(66\pi t + \frac{75}{64}\pi)$
$\alpha_y = 100\cos(66\pi t + \frac{75}{64}\pi)$

(j) `Sink`

$\ddot{p}_x = 10\sin(66\pi t)$
$\ddot{p}_y = 10\cos(66\pi t)$
$\alpha_x = 100\sin(66\pi t + \frac{11}{64}\pi)$
$\alpha_y = 100\cos(66\pi t + \frac{11}{64}\pi)$

(k) `Source`

$\alpha_z = 100\sin(66\pi t)$
$\alpha_y = 100\sin(66\pi t + \frac{1}{2}\pi)$

(l) `DivCircle`

Fig. 5. Numerically calculated asymptotic velocity fields corresponding to sinusoidal motion primitives. The fields are calculated for a point part with $\mu_k = \mu_s = 0.3$. Arrows are drawn in 2 cm increments. Arrows are missing in the corners of (h)–(k) because the part lost contact with the plate at those locations before reaching the asymptotic state. Linear accelerations are in m/s^2. Angular accelerations are in rad/s^2. All acceleration components have a frequency of 33 Hz. Overlaid on each asymptotic velocity field is a six second (200 cycle) simulation of a point part starting from rest incorporating the full system dynamics. The position of the part is plotted every 0.3 seconds (every 10 cycles).

speaker is connected to the plate with threaded aluminum rods and two compliant joints made of tygon tubing with $\frac{1}{2}$????? inch bend radius.

Four two-axis accelerometers (****)are mounted around the perimeter of the plate in increments of 60 or 120 degrees. The direction of the axes are shown in Figure **??**. We use a least squares approximation to determine $\ddot{\mathbf{p}}$ and $\boldsymbol{\alpha}$ from the eight accelerometer readings assuming that $\mathbf{R} = \mathbf{I}$, $\mathbf{p} = \mathbf{0}$, and $\boldsymbol{\omega} = 0$.

Two-axis accelerometers are also mounted on each speaker, but only acceleration in the vertical direction is measured.

Accelerometer signals are acquired by a PC running MATLAB xPC using a **** DAQ board sampling at 10,000*** Hz. Signals are sent to the amplifier using a *** DAQ board.

**Bode plots

A. Acceleration Control

A spectral decomposition learning control method appropriate for linear systems is used to control the plate's acceleration. The method entails converting all signals to the frequency domain, where the magnitude and phase of the desired and measured signals are compared at each frequency.

Let $Y(s)$ be the discrete Fourier transform of the numerical representation of the vector of measured acceleration components $y(t) = [\ddot{p}^d, \ddot{p}_y, \ddot{p}_z, \alpha_x, \alpha_x, \alpha_x]^T$ during one cycle. Let $D(s)$ be the discrete Fourier transform of the numerical representation of the vector of desired acceleration components $d(t) = [\ddot{p}_x^d, \ddot{p}_y^d, \ddot{p}_z^d, \alpha_x^d, \alpha_x^d, \alpha_x^d]^T$ during one cycle. Let $U(s)$ be the discrete Fourier transform of the numerical representation of the six control voltages sent to the speakers $u(t) = [V_1, V_2, V_3, V_4, V_5, V_6]^T$ during one cycle.

An initialization routine measures the plate's acceleration response to sinusoidal input voltages sent to one speaker for a range of frequencies. This process is then repeated for the other five speakers. From this data, we construct a discrete approximation to the system's six by six transfer function matrix $G(s)$, where $Y(s) = G(s)U(s)$. We use the iterative control law

$$U(s) \leftarrow U(s) + kG^{-1}(s)\left(D(s) - Y(s)\right), \qquad (24)$$

where $k = 0.05$, to drive the magnitude and phase of the plate's acceleration components at each frequency to their desired values. Figure 7 shows an example of the desired and measured acceleration profiles in the time domain for a sinusoidal motion primitive after 50 controller updates.

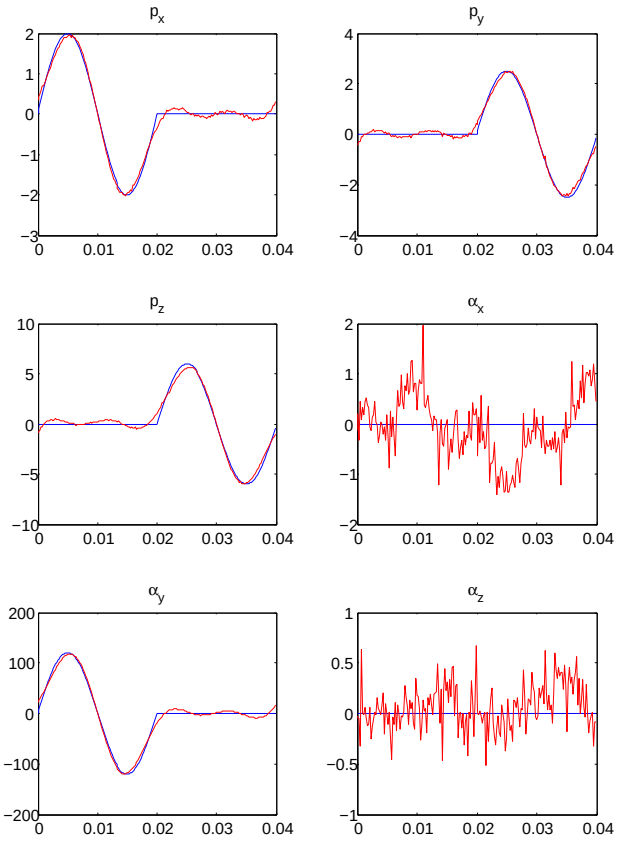

Fig. 7. TO BE REPLACED WITH SINUSOIDAL MOTION PRIMITIVE WITH LEGEND AND, LABELS, AND CORRECT ORDERING OF GRAPHS

B. results

superposition of videos and fields

X. Conclusions

extension to parts with planar extent
how to characterize the class of obtainable fields

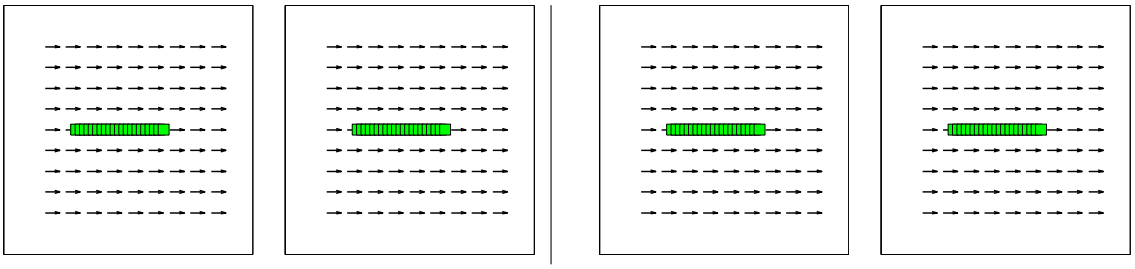

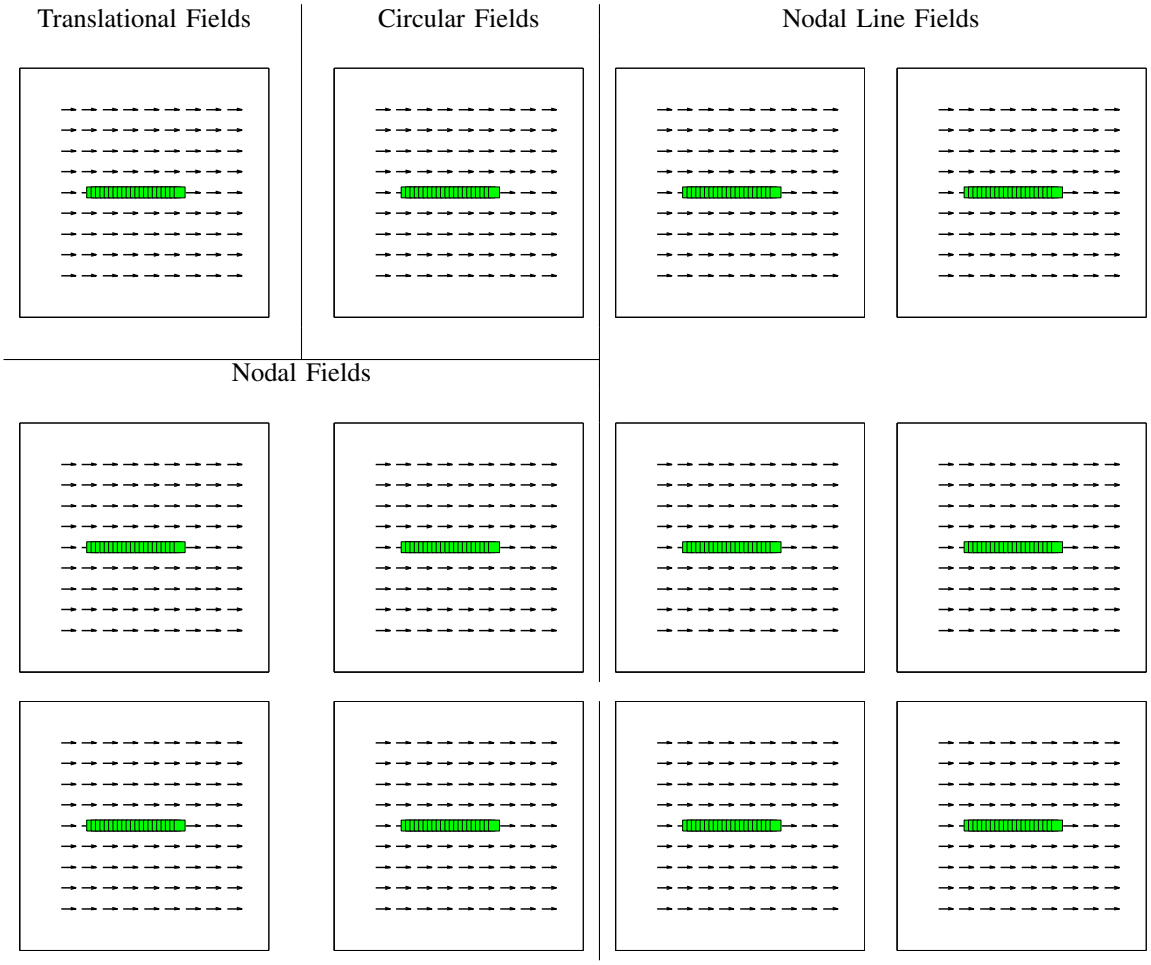
Translational Fields
Circular Fields
Nodal Line Fields
Nodal Fields